Total Cross Sections for High-Energy Neutrons*

VAUGHN CULLER AND R. W. WANIEK
Cyclotron Laboratory, Harvard University, Cambridge, Massachusetts
(Received April 4, 1955)

The total cross sections for high-energy neutrons have been determined for 12 elements (H, D, C, O, Al, Si, Cl, Ti, Fe, Cu, Hg, and Pb) for several points in the range between 60 and 110 Mev. The good-geometry attenuation experiment was conducted in the neutron beam produced by the bombardment of a beryllium target by the internal proton beam of the Harvard 95-in. synchrocyclotron. The angular and energy resolution permitted by the use of scintillation counter telescope techniques is discussed. Results are analyzed by using the optical model of the nucleus.

I. INTRODUCTION

THE values and the variations of total neutron cross sections as a function of incident neutron energy serve as a basis for comparison of various nuclear models, and, to this extent, permit the determination of nuclear radii. The cross sections in the region between 50 and 100 Mev are of special interest because the more rapid variation with energy indicates a transition effect in nuclear properties. From a phenomenological approach, this denotes a change from an opaque to a transparent nucleus. Additional interest is provided by the presence in this energy region of maxima in the cross section curves of high-Z elements. Thus, a precise knowledge of the values of total cross sections in this region is highly desirable. We therefore felt that cross sections should be examined with the good energy resolution afforded by scintillation counter techniques.

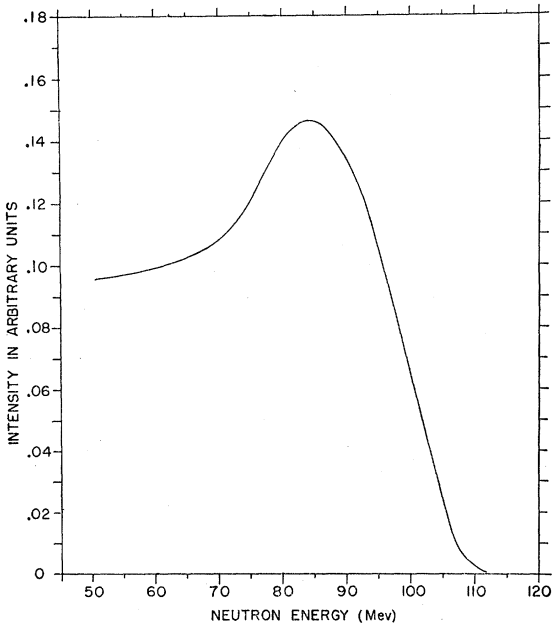

FIG. 1. Neutron spectrum produced in forward direction by internal proton beam bombardment of $\frac{1}{4}$-in. Be target in the Harvard 95-in. synchrocyclotron.

* Supported by the joint program of the Office of Naval Research and the U. S. Atomic Energy Commission.

II. GEOMETRY AND APPARATUS

(A) Source of Neutrons and Experimental Lay-Out

The high-energy neutron beam used in this experiment (Fig. 1) was produced in charge exchange collisions by an internal proton beam bombardment of a $\frac{1}{4}$ in. thick, 1.5 in. high beryllium target. The neutrons emitted in the forward direction were collimated by brass tubing of rectangular cross section (1.37 in. by 2.87 in.) placed in a 6-ft water tank in the cyclotron shielding (Fig. 2). The beam intensity was constantly monitored at the exit of this pipe by a coincidence counter telescope. Approximately 150 cm from the monitor scatterer the beam passed through the appropriate attenuators and continued then through a second collimator consisting of a pipe, similar to the first one, encased in a water jacket 4 feet long permanently cemented in a concrete cube 7 feet thick. At the exit of this second collimator a scintillation counter telescope was used to determine the neutron beam intensity for various energy bands.

(B) Monitor Telescope System

Originally[1,2] a triple-coincidence scintillation counter telescope served to monitor the neutron beam by counting recoil protons from a polyethylene scatterer. The telescope, composed of plastic scintillators mounted on 1P21 photomultipliers, was placed at an angle of 15° to the neutron beam. By comparison of its counting rate with the rates of the various channels of the counter telescope described in the next section, two things were noted. The first was that the telescope had a constant efficiency; the second was that there were shifts in the high energy region of the neutron spectrum. It was found that results with good internal consistency could be obtained if the beam intensity was steady and if no controls of the cyclotron were manipulated. In order to minimize the effects of any steady drift in the neutron beam spectrum data were taken in symmetric cycles. At least five such cycles were made for each energy band, cross sections being determined for each cycle and resultant values appropriately weighted and averaged.

[1] V. Culler and R. W. Waniek, Phys. Rev. **87**, 221 (1952).
[2] V. Culler and R. W. Waniek, Phys. Rev. **95**, 585 (1954).

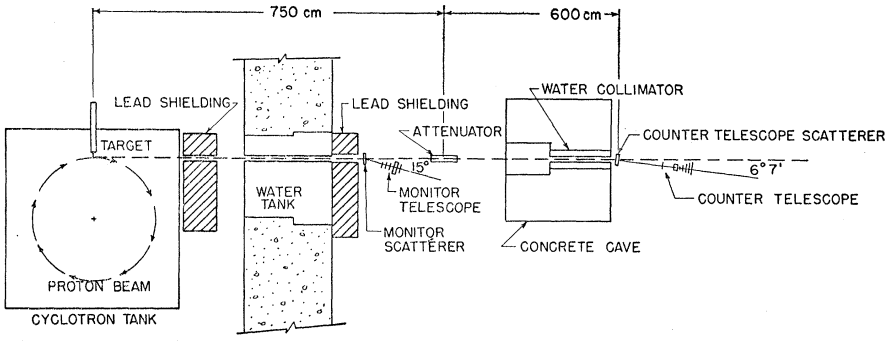

FIG. 2. Top view of experimental lay-out.

Later, in order to save running time as well as to get even more reliable data, a new monitor telescope with an added fourth counter was used. With this telescope suitable polyethylene absorbers were placed between the third and fourth counters so that the threshold energy for a recoil proton producing quadruple coincidence was about 85 Mev. The ratio of triple to quadruple coincidences then gave an indication of spectral changes. Any dubious counting cycles were rejected, the criterion for rejection being either beam intensity changes beyond about 15 percent or inconsistencies with the "empty-polyethylene" counts (no sample and a polyethylene scatterer in the counter telescope system) made at the beginning and at the end of each cycle. Rejections were made of the entire cycle in doubt before final results were calculated.

(C) Attenuators and Attenuator Changer

The solid attenuators were machined to four inches in diameter. The liquid and powder (silicon) attenuators were in containers machined to the same diameter. The containers had foil windows retained by "O" rings at each end. Whenever possible, lengths were chosen to be approximately two mean free paths, this length yielding about the best counting statistics in a given counting time.[3] The cross section of hydrogen was determined by a CH_2-C subtraction. In the measurement of the deuterium cross section which was determined by a D_2O-H_2O difference, the lengths of the containers were matched so that the oxygen components were nearly the same. During this rather long run intensity measurements were made also with no attenuator, thus permitting the determination of the cross section of oxygen by a H_2O-2H subtraction. The cross section of chlorine was determined by a CCl_4-C subtraction.

The areal densities of the solid samples were determined by measurements with micrometer calipers and analytical balances. Volume densities were also measured to ascertain the homogeneity of the samples. The areal density of the silicon was determined by measuring the inner diameter of the machined container and finding the difference between its "gross" and "tare" weights. The areal densities of the liquids were found by the use of hydrometers and the lengths of the containers. A recording thermometer was used to monitor the temperature in the area in which the attenuator changer was placed. Only negligible temperature changes existed. All samples, with the exception of titanium were pure to better than 99.5%. The titanium[4] was found to contain 3.2% Al, 3.3% Mg, and 0.10% C. The attenuator changer permitted the accurate alignment of three samples, and included a position for measuring the unattenuated beam. It was remotely operated from the control room with a reproducibility in each position of $\pm\frac{1}{16}$ in. from the central point.

(D) Counter Telescope System

The counter telescope system is composed of two sections and is pictured in Fig. 3. One section is the

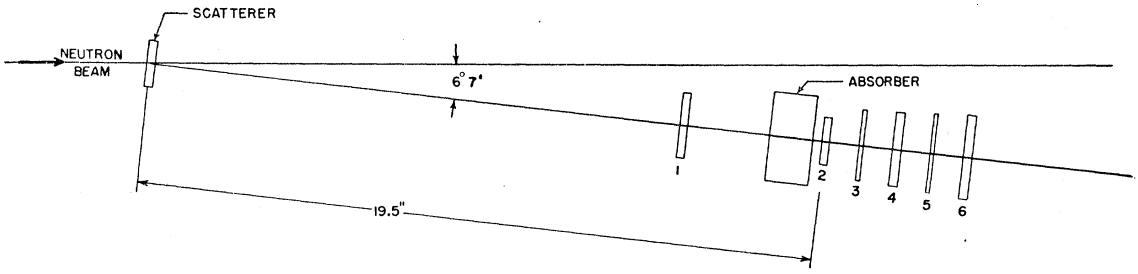

FIG. 3. Counter telescope system.

[3] M. E. Rose and M. M. Shapiro, Phys. Rev. **74**, 1853 (1948).
[4] The titanium sample was loaned by Rem-Cru Titanium Inc., Midland, Pennsylvania, through the auspices of Mr. A. E. Sylvester of Hawkridge Bros. Company, Boston, Massachusetts.

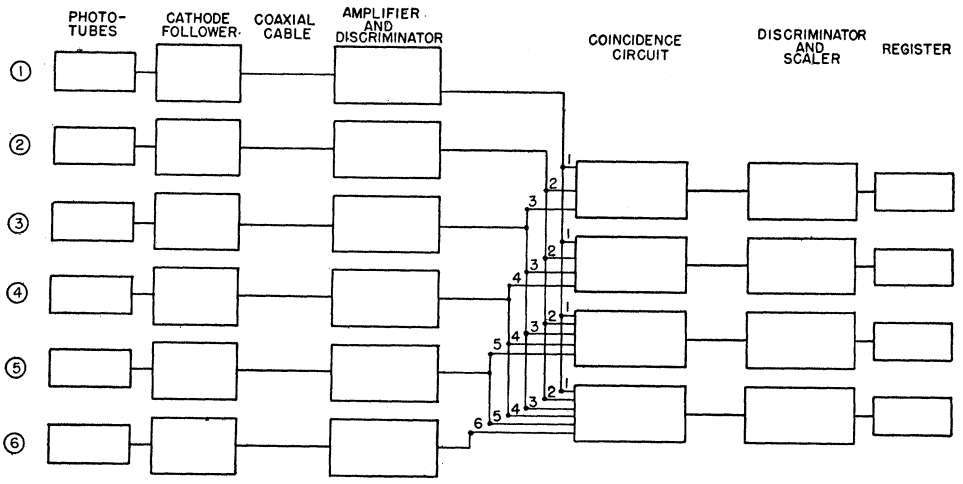

(a) Absorber telescope.

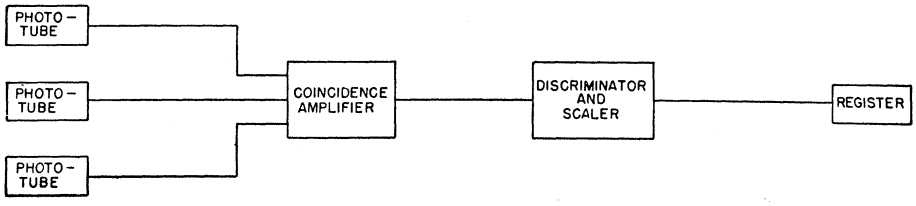

(b) Monitor telescope.

FIG. 4. Block diagram of electronic system.

counter telescope itself which is made up of 6 scintillation counters at a design angle of 6° 7′ to the neutron beam. The other section is a scatterer changer, operated remotely from the control room, which places a polyethylene or a carbon scatterer in the beam. In addition, a background or no-scatterer position is used.

The telescope consists of six plastic scintillators mounted on 1P21 multiplier phototubes. An aluminum stand supports the counters rigidly and permits careful alignment of the centers of the plastic scintillators so that the axis of the telescope can be made to fall at any given angle to the neutron beam. This angle is chosen as small as possible consistent with the necessity of keeping all counters out of the direct neutron beam, thus keeping the singles rate of every counter at a reasonable value. We estimate an error of less than $\frac{1}{4}°$ in positioning the telescope.

The choice of angle is indicated by $n-p$ scattering results and by energy resolution considerations. In the laboratory reference system, the differential cross section falls off rapidly with increasing angle, hence the choice of a small angle yields a higher counting rate for a given neutron beam intensity and counter size. The telescope utilized range differences to determine the energy of the recoil protons from the polyethylene scatterer. To achieve suitable energy bands polyethylene absorbers were placed in front of the defining crystal. In order to take advantage of the two-body scattering component due to the hydrogen in the scatterer, and thus uniquely determine the energy of the incident neutrons producing the recoils, it was necessary to subtract out the contribution due to carbon. This was done statistically by placing in the beam a carbon scatterer whose stopping power for the protons matched that of the polyethylene scatterer. Since this meant putting more carbon atoms per square centimeter in the neutron beam than did the polyethylene scatterer, only the proper fraction, f, of the proton intensity recoiling from the carbon scatterer was subtracted. This subtraction simultaneously removed the same fraction, f, of the background (no-scatterer) intensity. In order to account completely for this background a contribution $(1-f)$ of the intensity with no scatterer was also subtracted, thus getting only that portion of scattered protons for which the related neutron energy could be determined exactly, according to the relativistically correct formula:

$$E_p=\frac{E_n}{1+(1+E_n/2Mc^2)\tan^2\theta}, \tag{1}$$

where E_n is the neutron energy and E_p the energy of the recoil proton. For the energy region involved in this experiment, the expression reduces to

$$E_n=E_p/\cos^2\theta \tag{2}$$

with negligible error. This equation also indicates the choice of a small angle θ in order to minimize the dependence of energy on angular variation.

Pulses from each phototube are fed into a cathode follower and then through about 300 feet of RG62U coaxial cable (terminated by its characteristic im-

pedance) to a linear amplifier and then passed into a discriminator. The discriminator outputs are then fed into standard diode-type coincidence circuits which permit any combination of coinciding pulses to be recorded by conventional scalers and mechanical register. This equipment (Fig. 4) is in the cyclotron control room.

Coincidences from the first three, four, five, and all six counters are recorded, the difference counts yielding the number of protons stopping in the appropriate counter. The resolution of the entire system, up to the scalers, is better than one microsecond. The scalers have a resolution of about five microseconds, hence are sufficiently fast to cause no trouble since the coincidence rates are relatively low. Losses due to deadtime, multiple scattering of protons out of the telescope, and nuclear absorption were negligible. The efficiency of every counter was found to be essentially 100%. The entire system was frequently checked for stability and for over-all efficiency.

(E) Angular and Energy Resolution

In this type of experiment, angular resolution *per se* is only of slight importance since we are measuring a total rather than a differential cross section. The effect, however, of the angular resolution on the energy resolution must be taken into account as indicated by Eq. (2). Having decided on an angular resolution commensurate with the energy resolution requirements a few practical points in the design of this telescope may now be considered. The choice of small angles is dictated for best energy resolution consistent with the necessity of keeping the counters out of the direct neutron beam. This avoids both inordinately high singles counting rates and the high background coincidence rate caused by proton recoils produced by neutrons in the first counter. Therefore a preliminary experiment was made to determine just how well the beam could be collimated.

By using both photographic plates and counters as detectors, it was found possible to build a collimation system such that the beam spread at the exit of the system was essentially the one geometrically predicted by the size of the source and aperture system.

An arbitrary minimum distance was chosen for the defining crystal to clear the beam. In a plane perpendicular to the beam axis let us now visualize the projections of an arbitrarily shaped defining scatterer and defining crystal, one on each side of a band of width equal to our minimum separation distance. If both the scatterer and the crystal lie in planes orthogonal to the incident beam, then the tangent of the angle through which a particle is scattered is proportional to the distance between the two corresponding points in our projection. Some reflection will indicate that the optimum counting rate consistent with the angular resolution requirements is determined by the circle shown in Fig. 5. The diameter (D_θ) of this circle is proportional to the tangent of the maximum angle permitted by the criteria of angular resolution. The two segments in the circle would represent the ideal shapes for the scatterer and for the defining crystal. For practical purposes, though, we selected the rectangles of maximum inscribed area. The extension to a scatterer and crystal system of finite thickness is fairly obvious. The remainder of the telescope would appear to follow in a logical sequence, each crystal being parallel to the defining crystal and of sufficient size to cover the acceptance pyramid. Such a telescope, however, has a drawback due to the fact that two protons of a given energy but scattered at angular extremes would have sizeably different projected ranges, very possibly stopping in different crystals. The solution of this problem lies in a rotation of the scatterer and defining crystal so that the line through their centers is perpendicular to their faces. This is followed by either a graphical or an analytical determination of the sizes of the remaining crystals. In our specific case we felt it advisable to choose the collimating system rather than the scatterer as the defining source. We found that 1.5 in. by 3 in. o.d. wave guide of 0.064 in. wall thickness was sufficiently near the optimum rectangular shape. The scatterers were made somewhat larger in each dimension thus obviating the complication of precise positioning apparatus. We now have a defining system which satisfies two requirements: (1) it gives us definite minimum and maximum angles through which a particle may be scattered; (2) it gives us an optimized counting rate.

Especially if the angular acceptance interval is large we may wish to know more about what we may term the angular resolution function of the counter telescope. In other words, we may inquire as to the relative probability of seeing a particle scattered through some angle θ, and, since we know only that the origin of the

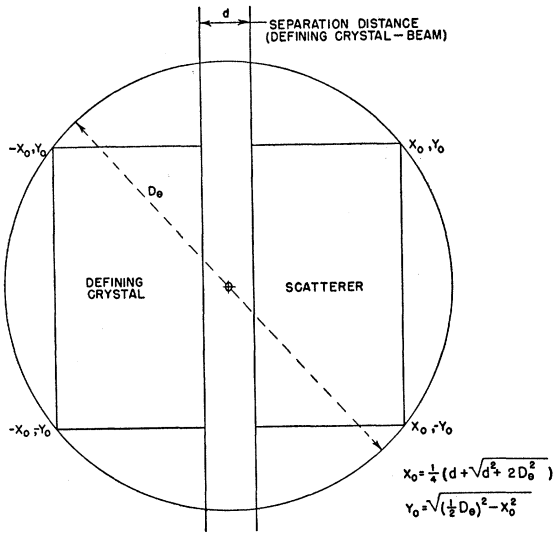

FIG. 5. Defining crystal-scatterer system.

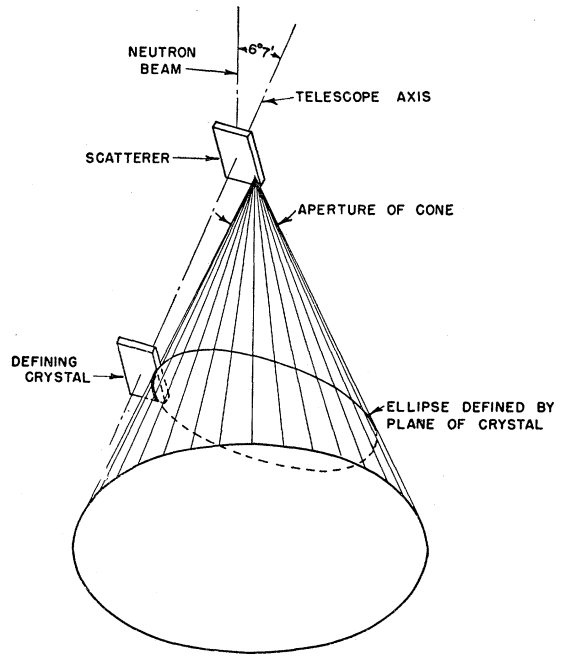

FIG. 6. Geometry for angular resolution calculations.

particle is somewhere in the scatterer, we must state this probability for the case of any two points in the scatterer being equally probable origins. We thus may define the angular resolution function of the telescope as being the function of scattering angle which states the relative probability of detection of the particle, in the case in which the particle has equal likelihood of being scattered in any angular interval θ to $\theta+d\theta$, θ being the angle between the trajectory of the scattered particle and the axis of the incoming beam.

In this case, then, we may think of the scattered flux from any point in the scatterer as being made up of cones with equal flux for equal angular intervals, the source point in the scatterer being the origin. Further, the cones are all right circular cones with axes parallel to the beam axis. Let us consider one such cone as illustrated in Fig. 6. Since the detector or defining counter is in a plane which is not orthogonal to the beam axis the section of the cone by this plane is either an ellipse or an hyperbola rather than a circle. The axis of the cone intersects this plane, therefore the section is an ellipse.

For the case in which the counter is not in a plane orthogonal to the beam axis but in a plane which is nearly so, the elliptical segments may be approximated as circular segments with small error. For a point source then, the angular resolution function is particularly easy to evaluate. It is simply the function of θ expressing the area of the counter cut off by the two cones of semivertex angles θ and $\theta+d\theta$ divided by the total area in the plane of the counter cut off by the same cones. Generalization to finite source (i.e., scatterer) may be approximated by subdividing the scatterer into sections of equal area, each of which is assumed characterized by a point source.

In the more general case in which the ellipses cannot be approximated as circles, we are faced with an alternative approach which is, of course, applicable to the simple case and which may actually be somewhat easier to use in practice. For a point source let us consider the circular sections made by the various cones in a plane perpendicular to the beam axis. Let us for convenience take this reference plane as being farther from the source than any similar plane through the defining counter: the angles of scattering are then uniquely related to the radius of the various circles. The angular resolution function is then the arc length "removed" by the defining counter divided by the circumference of the circle as a function of radius (i.e., scattering angle). Even more simply, by choosing the projected source point as the origin of a polar diagram the angular resolution function is then the polar angle subtended by the defining crystal as a function of radius (i.e., scattering angle). Since we know the exact intersection of the scattering cone with the counter, we may take the extreme points of intersection as reference points for the determination of this angle.

The actual mechanical procedure used may make this process more understandable. For a given source point we find the intersection with the defining counter of the cone of semivertex angle θ. This section or curve is

TABLE I. Total cross sections in units of 10^{-27} cm^2.

Neutron energy (Mev)	High-energy bands 93.4±0.5	97.2±1.0	101.1±0.5	106.8±2
H	77± 5	76± 3	80± 7	59± 16
D	110± 7	108± 5	81± 10	62± 22
C	518± 6	494± 4	466± 7	508± 18
O	721± 13	675± 9	649± 14	668± 42
Al	1067± 29	1046± 23	920± 50	1064±130
Si	1136± 52	1067± 42	1040± 90	925±220
Cl	1382± 58	1336± 40	1380± 75	1260± 90
Ti	1650± 41	1565± 29	1574± 54	1490± 80
Fe	1947± 48	1874± 37	1735± 80	1940±185
Cu	2204± 56	2023± 39	1880± 70	1935±110
Hg	4315±150	4450±105	4525±180	4540±255
Pb	4630± 90	4595± 65	4410±120	4740±210

Neutron energy (Mev)	Medium-energy bands 76.7±0.5	81.2±1.0	85.5±0.5	99.4±4
C	614± 31	585± 17	602± 19	518± 7
Cl	1420± 85	1597± 59	1371± 59	1332± 19
Ti	1760± 90	1900± 57	1772± 59	1628± 20
Cu	2150±100	2335± 65	2225± 70	2118± 23
Hg	4310±200	4985±150	4680±150	4697± 50
Pb	4590±225	4450±160	4650±195	4605±120

Neutron energy (Mev)	Low-energy bands 61.0±0.5	66.1±1.0	71.2±0.5	92.3±7
C	674± 62	671± 42	601± 41	520± 80
Ti	1905± 90	2210± 80	1880± 80	1737± 15
Cu	2440± 20	2495± 80	2450±103	2139± 18
Hg	3770±490	5000±400	5320±575	4765±120
Pb	4590±225	4550±160	4650±195	4605±120

elliptical. This ellipse intersects the counter in an even number of points. Each of these points determines a definite ray of the cone since the origin of the cone is fixed. The intersection of each of these rays with the reference plane is found. These new points necessarily lie on a circle. The appropriate arc lengths or angles subtended may then be easily measured to give the value of the angular resolution function for this value of the scattering angle θ.

The angular resolution function is weighted by the value of $\sin\theta$ at each point to give a new angular resolution function in terms of solid angle. The final angular resolution function is the appropriate sum of the "point source" angular resolution functions. We are now in a position to consider the effects of angular resolution on energy. The angular resolution function is first weighted by the differential $n-p$ cross section, modified because it is the proton and not the neutron which is seen by the telescope. A mean proton energy derived from range energy relations for the telescope is used to find the equivalent neutron energy for each angle, the angular resolution function as a result being transformed into an energy resolution function. Finally, this function is weighted by the spectrum of the incident neutron beam and a mean or effective neutron energy determined. In order to estimate the error in this mean neutron energy deliberate discrepancies may be introduced at any point. It was found that practically any step in this derivation could be dropped without shifting the effective neutron energy by more than about 0.2 Mev. On this basis the errors in the effective energies were calculated not to exceed those indicated in Table I. It should be pointed out that this procedure must be used carefully. If there are any very large fluctuations of any component with angle or energy the effective energy as well as resultant energy resolution could be affected.

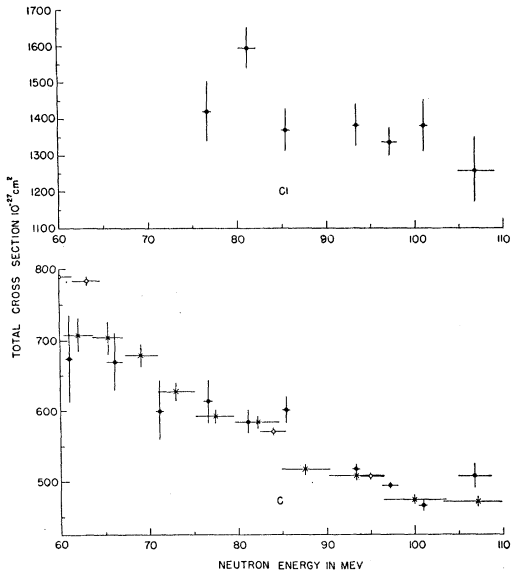

FIG. 7. Total cross sections of carbon and chlorine; Harvard results: ●, Harwell results: o, Berkeley results: ×.

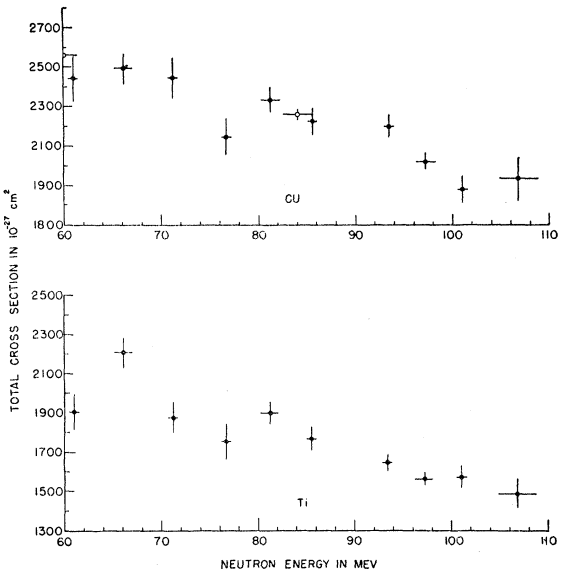

FIG. 8. Total cross sections of copper and titanium; Harvard results: ●, Harwell results: o.

III. EXPERIMENTAL PROCEDURES

The procedure of a typical measurement consisted in carefully aligning collimators, monitor and counter telescopes and the attenuator samples by means of a cathetometer aimed at the internal beryllium target. The monitor telescope was then checked for constant efficiency and the absolute efficiency of each of the counters in the counter telescope was determined. The requirements for the counter and for the related electronics were essentially 100% efficiency and phototube voltage near the center of an efficiency *versus* phototube voltage plateau. The runs were carried out in symmetric cycles, each being started and finished with a no-attenuator measurement of the intensity. A typical cycle was made up of the following beam intensity measurements: no-attenuator, sample A, sample B, sample B, sample A, no-attenuator. Each of these determinations was composed of measurements made with each of the possible scatterers (polyethylene, carbon and no-scatterer) for the reasons outlined in the section on the counter telescope system. The purpose of the symmetric cycles was to counterbalance partially the effects of long term cyclotron beam fluctuations which could have possibly affected the energy spectrum of the beam. The time apportioned to each measurement in the cycle was such as to yield optimum statistics for a given counting time. This required a preliminary cycle for each set of samples in order to ascertain the relative counting rates. The length of time allowed for each cycle was never more than 3 hours for several considerations. The most obvious one was the prevention of the loss of much data in the event of machine or

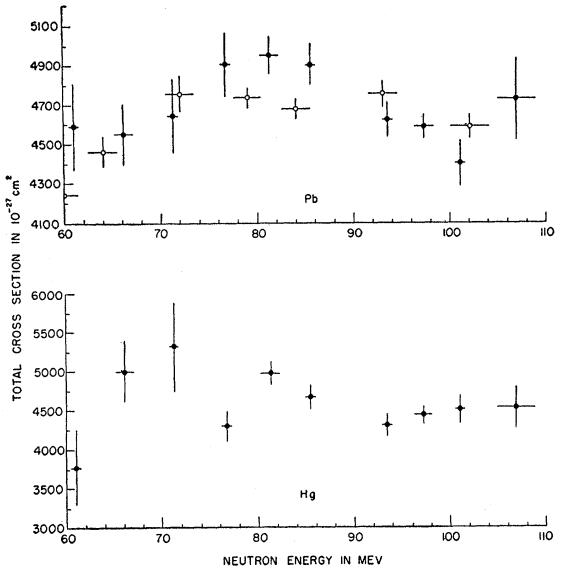

FIG. 9. Total cross sections of mercury and lead; Harvard results: ●, Harwell results: o.

equipment failure, the second was the beam drift possibility mentioned before and the third was to permit an easy check of the internal consistency of the data. In general, the cycles were repeated until a cross section with about 2.5% standard deviation was obtained.

IV. RESULTS AND ANALYSIS

The values of the cross sections are listed in Table I and are graphically presented in Figs. 7–10. Diffraction corrections were calculated either according to the theoretical procedure given by McMillan and Sewell[5] and outlined by Cook *et al.*[6] or, in the cases where experimental data was available, from the value of the differential elastic scattering cross section extrapolated to 0°.[7] The correction was about 1% for the heaviest elements, lead and mercury, and smaller for all others.

Corrections for impurities were negligible in every case, including that of titanium.

The cross sections of carbon and lead were taken with different thicknesses of sample material to check the exponential dependence of the absorption. This indicates the absence of beam degradation effects (increases in beam transmission due to in-scattered neutrons) other than those predicted by the diffraction correction.

The values at 106.8 Mev were taken at the extreme tail of the neutron spectrum where beam energy fluctuation effects and low counting rates impair the accuracy of the results. In this case the maximum energy of the neutrons (Fig. 1) defined the upper limit of the energy band, since this data was taken with the last counter of the telescope. This is also the case for the data at 92.3 and 99.4 Mev with the exception that wider energy ranges were used with a corresponding increase in counting rates.

The apparently low value in the cross section of deuterium at 101.1 Mev may possibly be attributed to counting errors.

For purposes of comparison, contemporaneous measurements made at Harwell[8] and at Berkeley[9] have been indicated in Figs. 7–10. This is the only data in this energy range, to our knowledge, taken with energy resolution comparable to ours, and the agreement is good. The maximum in the lead cross section falling at about 82 Mev appears to be defined more sharply than in the Harwell data. Comments on the significance of these peaks have been made by Lawson[10] although the situation is not completely understood.

It seems that future experiments with better absolute energy resolution and smaller counting errors are required to investigate the possibility of a more detailed structure. The total cross sections obtained in this

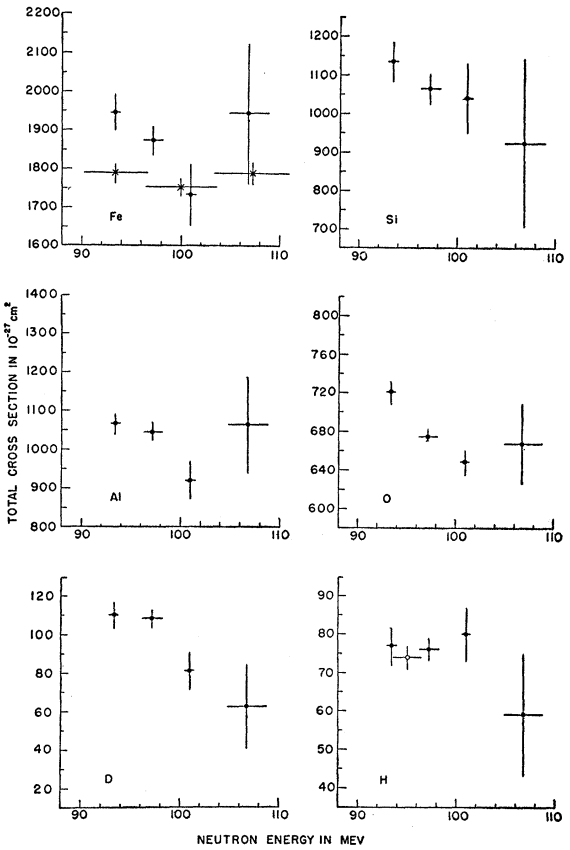

FIG. 10. Total cross sections of hydrogen, deuterium, oxygen, aluminum, silicon, and iron; Harvard results: ●, Harwell results: o, Berkeley results: ×.

[5] E. M. McMillan and D. C. Sewell, U. S. Atomic Energy Commission Report MDDC-1558, November, 1947 (unpublished).
[6] Cook, McMillan, Peterson, Sewell, Phys. Rev. **75**, 7 (1949).
[7] Bratenahl, Fernbach, Hildebrand, Leith, and Moyer, Phys. Rev. **77**, 597 (1950).
[8] A. E. Taylor and E. Wood, Phil. Mag. **44**, 95 (1953).
[9] B. Ragent, Phys. Rev. (to be published).
[10] J. D. Lawson, Phil. Mag. **44**, 102 (1953).

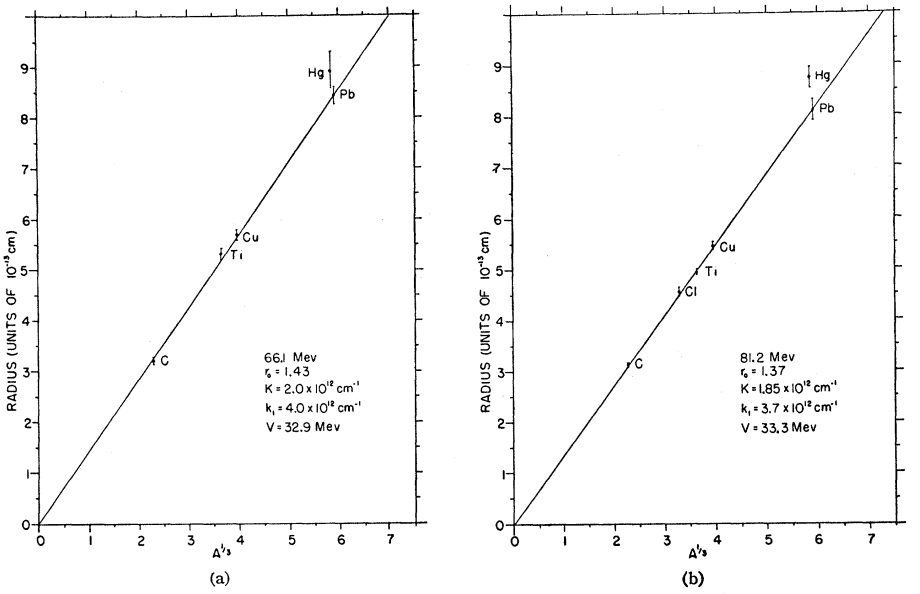

FIG. 11. Analysis of the experimental data at (a) 66.1 Mev, (b) 81.2 Mev, using the optical model of reference 11.

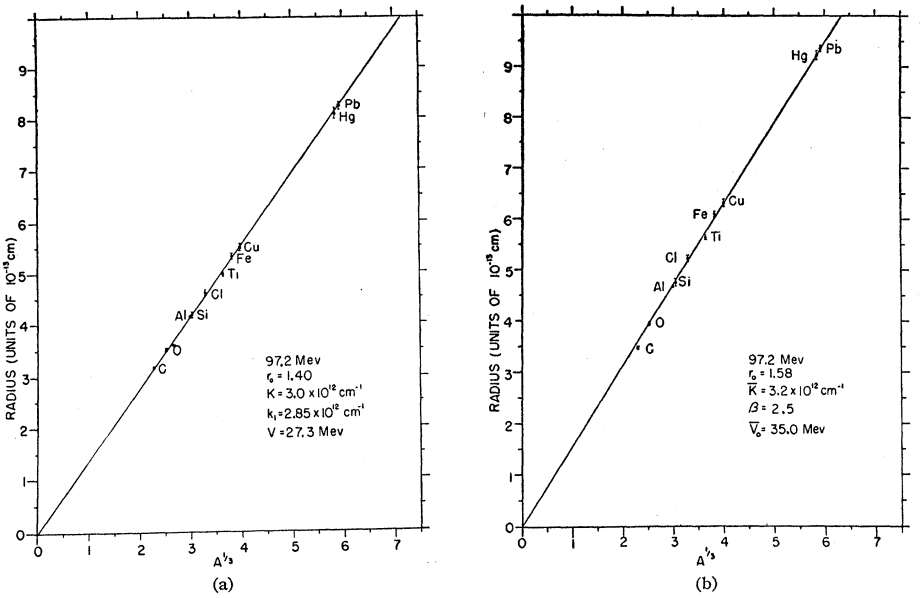

FIG. 12. Analysis of the experimental data at 97.2 Mev using (a) the optical model of reference 11, (b) that of reference 13.

experiment were used to investigate the reliability and the range of applicability of the theory describing the nucleus in terms of an analogy out of physical optics. The optical model[11,12] describes the nucleus as a sphere of uniform density, with an appropriate absorption coefficient and an index of refraction for the Schrödinger-de-Broglie neutron waves. The main limitation imposed is that the wavelength of the incident neutron should be much smaller than the nuclear radius, a high-energy approximation. This is already nearly the case for neutrons of several tens of Mev and will therefore hold even better around 100 Mev. This concept represents an oversimplification of a more realistic picture as it does not investigate any structural effects nor does it take care of interfacial reflections. The values of the propagation vectors outside and inside the nucleus, k and $k+k_1$, respectively, are calculated (the change in the phase velocity upon entering nuclear matter is related to the nuclear potential well of depth determined from the Fermi gas model of the nucleus). An absorption coefficient, K, is determined from the knowledge of $p-p$ and $n-p$ cross sections, the Pauli principle being taken into account. If we retain the expression,

$$R=r_0A^{\frac{1}{3}}\times10^{-13}\text{ cm}, \tag{3}$$

for the radius of a nucleus, it is necessary to use other than the predicted k_1 and K.

Best fitting values of k_1 and K are determined by an iteration procedure in which the nuclear radius obtained

[11] Fernbach, Serber, and Taylor, Phys. Rev. **75**, 1352 (1949).
[12] S. Fernbach, University of California Radiation Laboratory Report UCRL 1382, 1951 (unpublished).

from these parameters and the experimental data is plotted as a function of $A^{\frac{1}{3}}$, a straight line passing through the origin being required by Eq. (3). Figures 11(a), (b), and 12(a) represent the best results for the square nuclear potential well.

Heckrotte[13] has applied the optical model to a parabolically shaped nuclear well of maximum depth V_0. Figure 12(b) shows the best fit for the present data using this model. $\bar{K}$ is essentially the average value of K while β may be taken as 4/3 the quotient of the average value of k_1 and $\bar{K}$.

The fact that forced fittings of the data at 66.1 and 81.2 Mev, as well as similar fittings by two types of wells at 97.2 Mev are possible, serves to point out one of the strongest limitations of the present optical models, specifically that they do not yield unambiguously the dependence of total cross sections on neutron energy.

[13] W. Heckrotte, Phys. Rev. **95**, 1279 (1954).

V. ACKNOWLEDGMENTS

We should like to express our sincere appreciation to Professor N. F. Ramsey for his continued support and frequent discussions concerning the experiment. The aid of Mr. R. L. Smith was particularly valuable in curing all troubles of electronic nature, and Mr. R. H. Lambert should be thanked for the numerical calculations concerning the optical model.

Thanks are also due to Mr. M. J. Hurley and Mr. G. P. Weiss, as well as to the cyclotron staff.

PHYSICAL REVIEW VOLUME 99, NUMBER 3 AUGUST 1, 1955

Determination of the Strength Function of Nuclear Energy Levels*

S. E. DARDEN†
University of Wisconsin, Madison, Wisconsin
(Received March 28, 1955)

An investigation of the average reduced neutron width to spacing ratio, or strength function, $\langle\gamma_0^2\rangle/\bar{D}$, of nuclear energy levels has been carried out as a function of atomic weight and neutron energy. The experiment was performed by measuring deviations from exponential attenuation of a beam of neutrons passing through samples of various elements. Deviations from exponential attenuation were observed by comparing transmissions of thin samples for neutron beams filtered through thick samples with transmissions of thin samples for unfiltered beams.

1. INTRODUCTION

AMONG the features of the neutron-nucleus interaction which depend strongly on the nuclear model is the average neutron width to spacing ratio $\bar{\Gamma}_{nl}/\bar{D}$ of levels of the compound nucleus. For levels formed by neutrons of zero orbital angular momentum, the strong interaction model[1] predicts an average width to spacing ratio:

$$\bar{\Gamma}_{n0}/\bar{D}=2k\langle\gamma_0^2\rangle/\bar{D}\simeq 2k/\pi K, \qquad (1)$$

where k is the wave number of the emitted neutron and K is the wave number corresponding to the average kinetic energy of the neutron inside the nucleus. $\langle\gamma_0^2\rangle/\bar{D}$ is the average reduced neutron width to spacing ratio or strength function[2] for levels formed by S-wave neutrons. The complex square well model of Feshbach, Porter, and Weisskopf,[3] on the other hand, predicts sharp maxima in $\bar{\Gamma}_{n0}/\bar{D}$ as a function of atomic weight and energy. These maxima occur near the positions of the giant resonances attributed to S-wave neutrons in the average total cross sections.[4] Between peaks the predicted values of $\bar{\Gamma}_{n0}/\bar{D}$ fall to a fraction of the values expected from the strong interaction theory. Wigner, Lane, and Thomas[5] have come to similar conclusions concerning the reduced width density $\langle\gamma_l^2\rangle/\bar{D}$ of levels formed by neutrons having l units of orbital angular momentum. They have interpreted the giant resonances in the average total cross sections in terms of oscillations, over wide energy and atomic weight intervals, of $\langle\gamma_l^2\rangle/\bar{D}$.

Carter *et al.*[6] have performed a survey of slow neutron resonance parameters for nuclei having atomic weights between 100 and 200 in an attempt to investigate the dependence of $\langle\gamma_0^2\rangle/\bar{D}$ on atomic weight. Their results show a maximum in $\langle\gamma_0^2\rangle/\bar{D}$ for values of A near 160, in agreement with the predictions of the complex square well model. A similar collection of data which show a maximum in $\langle\gamma_0^2\rangle/\bar{D}$ for elements having atomic weight near 55 has been reported.[7] However, the in-

* Work supported by the U. S. Atomic Energy Commission and the Wisconsin Alumni Research Foundation.
† National Science Foundation Predoctoral Fellow.
[1] Feshbach, Peaslee, and Weisskopf, Phys. Rev. **71**, 145 (1947); V. F. Weisskopf, Helv. Phys. Acta **23**, 187 (1950).
[2] R. G. Thomas, Phys. Rev. **97**, 224 (1955).
[3] Feshbach, Porter, and Weisskopf, Phys. Rev. **96**, 448 (1954).
[4] H. H. Barschall, Phys. Rev. **86**, 431 (1952); R. K. Adair, Phys. Rev. **94**, 737 (1954).
[5] Wigner, Lane, and Thomas, Phys. Rev. **98**, 693 (1955).
[6] Carter, Harvey, Hughes, and Pilcher, Phys. Rev. **96**, 113 (1954).
[7] R. Cote and L. M. Bollinger, Phys. Rev. **98**, 1162(A) (1955).